

Mean field superconductivity approach in two dimensions: Hydrogen in Graphite

N. García^{1,2,*} and P. Esquinazi^{1,†}

¹*Division of Superconductivity and Magnetism, Institut für Experimentelle Physik II, Universität Leipzig, Linnéstraße 5, D-04103 Leipzig, Germany*

²*Laboratorio de Física de Sistemas Pequeños y Nanotecnología, Consejo Superior de Investigaciones Científicas, E-28006 Madrid, Spain*

Within the BCS theory of superconductivity we calculate the superconducting gap at zero temperature for metallic hydrogen-graphene system in order to estimate the superconducting critical temperature of quasi two dimensional highly oriented pyrolytic graphite. The obtained results are given as a function of the hydrogen-induced density of carriers n and their effective mass m^* . The obtained gap shows a Maxwell-like distribution with a maximum of ~ 60 K at $n \sim 3 \times 10^{14}$ cm⁻² and $m^*/m = 1$. The theoretical results are discussed taking into account recent experimental evidence for granular superconductivity in graphite.

PACS numbers: 74.10.+v, 74.20.-z

I. INTRODUCTION

Since the discovery of high temperature superconductivity¹ we learned that low dimensional structures are good candidates for high critical superconducting temperature T_c ². Related to this dimensionality effect it appears appropriate to mention also the role played by two dimensional (2D) interfaces in triggering superconductivity in nominally non-superconducting environment^{3,4,5}. One of the main paradigms for 2D carrier systems, graphene as well as highly oriented pyrolytic graphite (HOPG) or multigraphene have attracted considerable attention recently, partially due to the possibility of regulating the carrier density n by the field effect^{6,7}. On the other hand, hints for the existence of superconductivity in HOPG have been published in the last years^{8,9}.

Let us first point out some interesting aspects of multigraphene that should play a role in triggering the superconductivity phenomenon. Whereas graphene should be nominally a 2D system, multigraphene or HOPG is a quasi-2D system due to the weak coupling between graphene layers, which is the reason for the huge anisotropy in resistivity, for example¹⁰. Both materials, graphene as well as HOPG have high energetic phonons going up to ~ 0.15 eV with many other branches at lower energies^{11,12}. High energy phonons due to small element mass provide an excellent condition for superconductivity as in the case of metallic H at high pressures¹³. From this point of view it seems reasonable to look for superconductivity in these materials taking into account the whole phonon spectral function weighted by the electron-phonon coupling¹⁴.

For HOPG it has been recently shown that upon temperature (and defect concentration) $n \sim 10^8 \dots 10^{12}$ cm⁻².¹⁵ The lowest value obtained in clean samples and at low temperatures is clearly smaller than in free-standing as well as fixed-on-substrate graphene samples. To achieve a clear increase in the carrier density the case of attached hydrogen in HOPG is of spe-

cial interest. According to theoretical results upon the amount and the way hydrogen is attached to a graphene layer, a semiconducting, metallic or even a magnetically ordered state appears^{16,17,18}. In case of metallization the electron density may increase dramatically in the region near hydrogen, e.g. 0.1 to 1 electron per unit cell. Added to this effect, the effective mass increases from the usual very small values $m^* \lesssim 0.01m$ to nearly the free electron mass m ¹⁷. Note that in this case no Dirac dispersion relation is valid for graphite carriers but the usual quadratic one, dispersion that we will assume through all this work. The hydrogen-graphene bound system is interesting due to the influence in the spectral density similarly to the case of superconductivity in aromatic molecules^{14,19}.

On the other hand, we know that the reaction of hydrogen adsorbed on carbon is endothermic and difficult to realize. However, experimental results indicate large amounts of hydrogen is present in HOPG samples²⁰. Hydrogen in HOPG might be included through the synthesis of this material, obtained after high-pressure and high-temperature treatment of polymers (e.g. kapton) foils. We expect therefore hydrogen can be bounded to carbon, specially around vacancies and other defects, or at the interfaces conforming regions or pockets with different electron densities. Hydrogen bounded at defects might be the origin for the ferromagnetic properties^{21,22}, the anomalous transport observed in HOPG in the last years¹⁰ and for the existence of non-homogeneous, granular-like superconductivity⁹, possible at the interfaces between highly crystalline graphite regions in HOPG samples²³.

The purpose of this work is to calculate the superconducting energy gap at $T = 0$ K for a graphene layer and extend this result to the anisotropic graphite case. Following the Mermin-Wagner theorem in a pure 2D system there is no superconductivity²⁴ and therefore the problem should be treated as a Beresinskii-Kosterlitz-Thouless (BKT) phase transition^{25,26}. In the anisotropic case the problem is solved having a small anisotropy ϵ , which resembles the low coupling between graphene layers in graphite. As in the 2D anisotropic Heisenberg model, no matter how small is ϵ , one has an appreciable

critical temperature because of the logarithmic behavior of the thermal fluctuation influence^{27,28}. The results of this work indicate that hydrogen could play a decisive role triggering high temperature superconductivity in graphite.

II. SUPERCONDUCTIVITY AT HIGH METALLIC DENSITY OF CARRIERS

The estimate of the critical temperature T_c using BCS is done from the energy gap equation given by^{29,30}

$$\Delta(E) = -N(0) \int dE' V(E-E') \Delta(E') (1-2f(E')) / 2E', \quad (1)$$

where $N(0)$ is the density of states at the Fermi energy E_F , $V(E-E') = V_P(E-E') + V_C$ is the interaction potential that we split into the electron-phonon term and the Coulomb potential, this last taken as a constant for a given carrier density. The potential $V_P(E-E')$ depends on the pair-interaction-assisted phonon energy $E-E'$. Both potentials will be estimated below. Finally the Fermi-Dirac distribution function $f(E')$ at a given T that we set at T_c .

At high metallic densities $E_F \gg E_D$ (this last the Debye energy) T_c is estimated assuming that electron pairs are formed with an energy difference up to E_D around E_F . Then, the well known equation for the zero temperature energy gap (weak coupling limit)^{14,29,30}

$$\Delta(T=0) \approx 2E_D \exp(-1/(\lambda - \mu^*)), \quad (2)$$

is obtained with $\lambda = N(0) \langle V_P \rangle$ and

$$\mu^* = \mu / (1 + \mu \ln(E_F/E_D)), \quad (3)$$

with $\mu = N(0) \langle V_C \rangle$ where the $\langle \dots \rangle$ means the average within E_F or E_D and the screening length of the corresponding potentials. The well known result (2) is obtained solving Eq. (1) by introducing cutoffs energies for electrons and phonons. Using an Einstein approximation Morel and Anderson obtained the same results for $\Delta(0)$, λ and μ^* without introducing cutoffs³¹. The results remain the same for a 2D system but due to the BKT phase transition it is valid only at $T = 0$ K.

III. ESTIMATE OF $\Delta(0)$ IN 3D AND 2D AS A FUNCTION OF CARRIER DENSITY n

We discuss now the differences between 2D and 3D. We express all the necessary quantities as a function of r_s , the distance between the carriers in units of the Bohr radius. The quantities $q_F(r_s) = 1.91/(a_B r_s)$ and $q_T(r_s) = 1.38/(a_B \sqrt{r_s})$ are the 3D values for the Fermi vector and the inverse of the Thomas-Fermi decay length. Analogously for 2D we have $\sqrt{2}/(r_s a_B)$ and $2/a_B$. Notice that the inverse decay length in 2D does not depend

on the density $n = (\pi)^{-1}(a_B r_s)^{-2}$. Another important difference is in the Coulomb interaction that behaves as

$$V_C(q) = \frac{4\pi e^2}{q^2 + q_T^2(r_s)}, \quad (4)$$

for 3D and

$$V_C(q) = \frac{e^2}{2(q + q_T(r_s))}, \quad (5)$$

for 2D, where q is the wave vector. These potentials should be reliable for $r_s \lesssim 15$ above which Pines³² noted that convergence problems in the estimates may occur. Note that the value $r_s = 15$ is still smaller than those needed for the Wigner crystal formation^{33,34}.

In the 3D case the values of λ and μ in Eqs. (2) and (3) are given by

$$\lambda = \frac{r^2}{2(1+r^2)}, \quad (6)$$

$$\mu = \frac{r^2 \ln((1+r^2)/r^2)}{2}, \quad (7)$$

where $r^2 = (q_T(r_s)/2q_F(r_s))^2$. The Eqs. (6,7) correspond exactly to Eqs. (46,44) from Ref. 31. Note that our Eq. (7) is the average angular value of Eq. (26) of Ref. 31 that missed a factor r^2 in the corresponding Eq. (44). For the case of 2D we have μ as the average angular of the Coulomb potential

$$\mu = \frac{q_T}{4q_F} \int_0^{2q_F} \frac{1}{q + q_T} dq \quad (8)$$

$$= \frac{q_T}{4q_F} \ln \left(\frac{2q_F + q_T}{q_T} \right), \quad (9)$$

and λ is calculated as the average angular value of the square Coulomb potential multiplied by 0.66 because of averaging the q -moment. Therefore we have

$$\lambda = 0.66 \left(\frac{q_T}{2q_F} \right)^2 \int_0^1 \left(\frac{1}{(q_T/2q_F) + x} \right)^2 dx \quad (10)$$

$$= 0.66 \frac{q_T^2}{2q_F} \left(\frac{1}{q_T} - \frac{1}{q_T + q_F} \right). \quad (11)$$

Now we are prepared to estimate the values of $\Delta(0)$ in 2D and 3D for different values of r_s , a function of the electronic density. It should be notice that λ and μ obtained as defined previously agree with the values obtained by Morel and Anderson³¹. They obtained them including an Einstein effective frequency as approximation for the phonon structure. Within a Debye model similar equations are obtained but the phonon contribution is taken as an average on the whole phonon spectra.

We found that $\Delta(0)$ is in general about 10...100 times larger in 2D than in 3D at similar values of r_s . In Fig. 1 we present $\Delta(0)$ vs. r_s for the 3D case for 3 values of m^* corresponding to 0.1, 1 and 3 the free electron mass. Figure 2 shows the results for the 2D case. What can be the

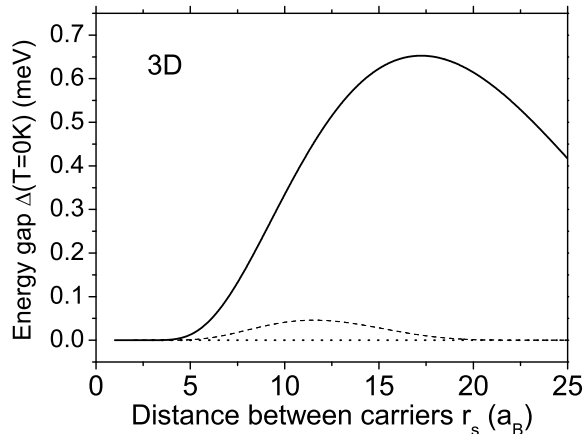


FIG. 1: Energy gap at $T = 0$ K vs. the distance between carriers r_s in units of Bohr radius $a_B = 4\pi\epsilon_0\hbar^2/m^*e^2$ for the 3D case and for the effective masses $m^* = 3, 1, 0.1$ of the free electron mass (continuous, dashed and dotted lines, respectively). The curves were obtained using Eqs. (2,3,4,6,7) and the parameter $E_D = k_B 860$ [K] as an average over all frequencies.

physical reasons for having energy gaps much larger in 2D than in 3D? They are related to the different weights and values of the ratios $q_T/2q_F$ and q_T/q_D (q_D is the averaged maximum phonon wave vector). Their contributions in 2D are dominant and depend on the effective mass, as seen in Fig. 3 where we plot the values of $q_T/2q_F$ and q_T/q_D , with $q_D = 10^8$ cm $^{-1}$ for 2D (as in 3D). Note that the differences in $\Delta(0)$ between the 2D and 3D cases are larger the smaller the effective mass m^* .

It is adequate to study quasi 2D problems with a degree of anisotropy provided by the ratio between the conductance in the atomic lattice plane and perpendicular to it, i.e. $\epsilon \simeq \sqrt{\sigma_c/\sigma_{ab}}$. For example, in the case of HOPG we have an in-plane conductance $\gtrsim 10^4$ than the conductance perpendicular to the plane. As in the case of the Heisenberg model in 2D with anisotropy, even if it is small, this is very effective to recover again the superconducting phase transition at $T > 0$ K by a logarithmic function of this anisotropy, i.e. $T_c \propto 1/\ln(K(1-\epsilon)) \propto -1/\ln(\epsilon)$ for $\epsilon \rightarrow 0$, where $K(x)$ is the elliptic function^{27,28}. The anisotropy produces a variation of T_c of $\sim 10-20\%$ of the value obtained from the simple estimate using the BCS result $T_c \sim 2\Delta(0)/(3.5k_B)$. Therefore the value of $\Delta(0)$ remains a good approximation for the anisotropic quasi 2D case.

We performed first calculations for HOPG at relatively low densities. We note that in graphene as well as in HOPG the expected T_c is negligible small at electron densities $n < 10^{13}$ cm $^{-2}$. According to the BCS approach and our estimates neither materials can be su-

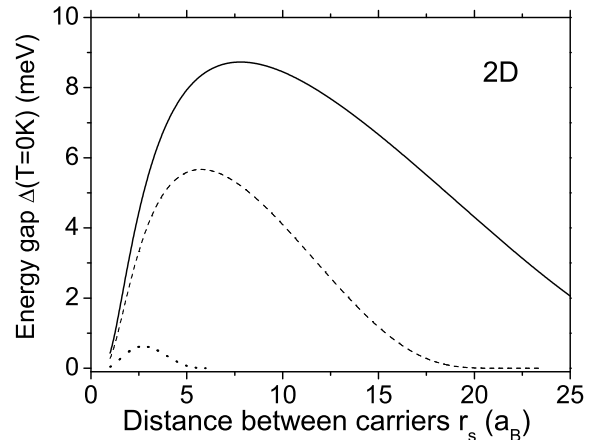


FIG. 2: The same as in Fig. 1 but for the 2D case with the same parameters.

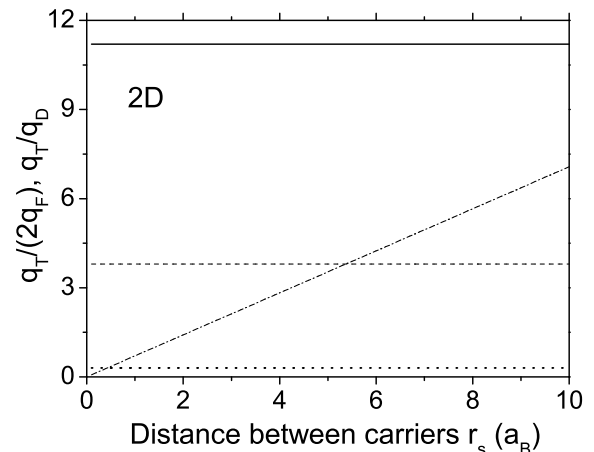


FIG. 3: Thomas-Fermi wavevector ratios $q_T/2q_F = r_s/\sqrt{2}$ (dashed-dotted line) and q_T/q_D for the 2D case for the three different effective masses 3, 1 and 0.1 of the free electron mass (continuous, dashed and dotted lines).

perconductors at those electron densities. However, for the electron densities obtained for the case of hydrogen fixed in special (e.g. Stone-Wales) defects we have $n \sim 10^{14} \dots 3 \times 10^{14}$ cm $^{-2}$ with a metallic-like band character that crosses the Fermi level with $m^* \sim m^{17}$. The estimated critical temperatures for these densities are around 25 K, values comparable to the observations in multigraphene samples^{9,23}. Note that decreasing n by a factor of two increases T_c approximately by a similar factor, see Fig. 2. According to our estimate, a further

decrease of n , however, would produce a decrease of the critical temperature, see Fig. 2.

Although defects in the graphene/graphite structure would increase the carrier density in a first stage, we believe that attached hydrogen may be the most probable reason for the local increase of n . The idea that hydrogen may trigger superconductivity in graphite due to the large increase in the electron density provides also a way to understand several experimental facts that we summarize below. Experimental results from SQUID^{8,35,36} and magnetotransport^{9,10} indicate that the possible superconducting state in HOPG has granular character: neither percolation in transport nor Meissner effect are observed so far for samples larger than $\sim 10 \mu\text{m}$. Irreversibilities in the magnetotransport of mesoscopic multigraphene samples⁹ are compatible with the existence of superconducting patches connected by semiconductor regions, similar to those irreversibilities observed in granular high-temperature superconductors³⁷. Transport measurements at different regions of the same micrometer small and a few tens of nanometers thick multigraphene samples reveal an inhomogeneous behavior compatible with the existence of metallic- and semiconductor-like regions⁹. Compatible with this view of HOPG, electric field force microscopy (EFM) measurements on its surface indicate the existence of large variations in the electronic potential providing a clear hint that HOPG is an inhomogeneous electronic system³⁸. A recently done correlation between the thickness dependence of the resistivity and magnetotransport with the internal microstructure of HOPG suggests that the internal interfaces between crystalline graphite regions are the regions where superconductivity can be located²³. These interfaces may have enough hydrogen trapped to increase the electronic density, triggering superconductivity in different regions with different critical temperatures, keeping the quasi-two dimensionality in agreement with the large anisotropy observed in the experiments⁹.

We should mention other approaches that deal with superconductivity in graphene and graphite. Starting with graphene^{39,40} we would like to note that for a carrier density $n < 10^{13} \text{ cm}^{-2}$ the critical temperature $T_c < 10^{-5} \text{ K}$.

Therefore, one needs to increase drastically the electron concentration in order to have a T_c in the few Kelvin range. Another publication⁴¹ obtains very large numbers for T_c in graphite. The basis of this result is to add certain atoms to graphite, in particular sulfur. The attractive interactions between electrons are based in electronic correlations effects. It is basically the same type of approach that we use but with phonons. It is clear that to produce superconductivity in graphite one has to incorporate a material into its planes to reise the carrier density to $\sim 10^{14} \text{ cm}^{-2}$. Otherwise we find that no appreciable superconductivity can be expected in graphite within the mean field approach.

IV. CONCLUSION

In conclusion, the superconducting-like behavior observed in bulk HOPG as well as in mesoscopic multigraphene samples could be explained applying the known techniques within the BCS approach and calculating $\Delta(0)$ for the quasi-2D problem. From our results we expect clear variations of T_c with the electronic density, indicating that neither perfect HOPG nor perfect graphene could be superconducting. We have presented results that indicate a huge increase in T_c for the 2D case with respect to the 3D for the same set of parameters. This is due to the behavior of $q_T(r_s)$ and $q_F(r_s)$ providing much higher values for $\Delta(0)$ in the 2D case. We have applied the BCS approach to the system graphene-hydrogen and have found that $\Delta(0) \gtrsim 25 \text{ K}$ are possible with reasonable electronic densities. Upon effective mass and electronic density, high critical temperatures in HOPG-hydrogen system may be realized and therefore the problem of superconductivity in graphite should be taken with more attention.

We gratefully acknowledge the support of the DAAD under Grant No. D/07/13369 (“Acciones Integradas Hispano-Alemanas”). One of us (P.E.) acknowledges discussions with Y. Dagan. One of us (N.G.) is supported by the Leibniz Professor fellowship of the University of Leipzig.

* Electronic address: nicolas.garcia@fsp.csic.es

† Electronic address: esquin@physik.uni-leipzig.de

¹ J. G. Berdnorz and K. A. Müller, *Z. Phys. B* **64**, 189 (1986).

² H. R. Ott, *in Superconductivity* (K. H. Bennemann and J. B. Ketterson (eds.), Springer Verlag, 2008), vol. 2, chap. 14, pp. 765–823.

³ A. Gozar, G. Logvenov, L. F. Kourkoutis, A. T. Bollinger, L. A. Giannuzzi, L. A. Muller, and I. Bozovic, *Nature* **455**, 782 (2008).

⁴ F. Muntyanua, A. Gilewski, K. Nenkov, J. Warchulska, and A. Zaleski, *Phys. Rev. B* **73**, 132507 (2006).

⁵ F. Muntyanua, A. Gilewski, K. Nenkov, A. Zaleski, and V. Chistol, *Solid State Commun.* **147**, 183 (2008).

⁶ K. S. Novoselov, A. K. Geim, S. V. Morozov, S. V. Dubonos, Y. Zhang, and D. Jiang, *Science* **306**, 666 (2004).

⁷ Y. Zhang, J. P. Small, W. V. Pontius, and P. Kim, *Appl. Phys. Lett.* **86**, 073104 (2005).

⁸ Y. Kopelevich and P. Esquinazi, *J. Low Temp. Phys.* **146**, 629 (2007), and refs. therein.

⁹ P. Esquinazi, N. García, J. Barzola-Quiquia, P. Rödiger, K. Schindler, J.-L. Yao, and M. Ziese, *Phys. Rev. B* **78**, 134516 (2008).

¹⁰ Y. Kopelevich, P. Esquinazi, J. H. S. Torres, R. R. da Silva, and H. Kempa (Springer-Verlag Berlin, 2003), vol. 43 of *Advances in Solid State Physics*, B. Kramer (Ed.), pp. 207–222.

¹¹ R. Nicklow, N. Wakabayashi, and H. G. Smith, *Phys. Rev.*

- B **5**, 4951 (1973).
- ¹² S. Siebentritt, R. Poes, K.-H. Rieder, and A. M. Shikin, Phys. Rev. B **55**, 7927 (1997).
- ¹³ N. W. Ashcroft, Phys. Rev. Lett. **21**, 1748 (1968).
- ¹⁴ K. H. Bennemann and J. B. Ketterson, eds., *Superconductivity* (Springer Verlag, 2008).
- ¹⁵ N. García, P. Esquinazi, J. Barzola-Quiquia, B. Ming, and D. Spoddig, Phys. Rev. B **78**, 035413 (2008).
- ¹⁶ O. V. Yazyev and L. Helm, Phys. Rev. B **75**, 125408 (2007), see also O. V. Yazyev, Phys. Rev. Lett. **101**, 037203 (2008).
- ¹⁷ E. J. Duplock, M. Scheffler, and P. J. D. Lindan, Phys. Rev. Lett. **92**, 225502 (2004).
- ¹⁸ L. Pisani, B. Montanari, and N. Harrison, New Journal of Physics **10**, 033002 (2008).
- ¹⁹ V. Z. Kresin and S. A. Wolf, *Fundamentals of Superconductivity* (Plenum Press, New York, 1990).
- ²⁰ P. Reichart, D. Spemann, A. Hauptner, A. Bergmaier, V. Hable, R. Hertenberg, C. Greubel, A. Setzer, T. Butz, G. Dollinger, et al., Nucl. Instrum. Methods Phys. Res. B **249**, 286 (2006).
- ²¹ P. Esquinazi, A. Setzer, R. Höhne, C. Semmelhack, Y. Kopelevich, D. Spemann, T. Butz, B. Kohlstrunk, and M. Lösche, Phys. Rev. B **66**, 024429 (2002).
- ²² J. Barzola-Quiquia, P. Esquinazi, M. Rothermel, D. Spemann, T. Butz, and N. García, Phys. Rev. B **76**, 161403(R) (2007).
- ²³ J. Barzola-Quiquia, J.-L. Yao, P. Rödiger, K. Schindler, and P. Esquinazi, phys. stat. sol. (a) **205**, 2924 (2008).
- ²⁴ N. D. Mermin and H. Wagner, Phys. Rev. Lett. **17**, 1133 (1966).
- ²⁵ V. L. Berezinskii, Zh. Eksp. Teor. Fiz. **59**, 907 (1970).
- ²⁶ L. Kosterlitz and D. Thouless, J. Phys. C **6**, 1181 (1973).
- ²⁷ A. P. Levanyuk and N. García, J. Phys.: Condens. Matt. **4**, 10277 (1992).
- ²⁸ E. Brezin and J. Zin-Justin, Phys. Rev. B **14**, 3110 (1976).
- ²⁹ P. G. de Gennes, *Superconductivity of metals and alloys* (Perseus Books Publishing, 1999).
- ³⁰ N. N. Bogoluibov and V. V. Tomachez, *A new Method in Theory of Superconductivity* (Consultant Bureau Inc. New York, Chapman and Hall LTD, London, 1959).
- ³¹ P. Morel and P. W. Anderson, Phys. Rev. **125**, 1263 (1962).
- ³² D. Pines, *Electron Interactions in Metals Solids*, vol. 1 of *Solid State Physics* (Academic Press, 1955).
- ³³ E. Wigner, Phys. Rev. **46**, 1002 (1934).
- ³⁴ B. Tanatar and D. M. Ceperly, Phys. Rev. B **39**, 5005 (1989).
- ³⁵ Y. Kopelevich, P. Esquinazi, J. Torres, and S. Moehlecke, J. Low Temp. Phys. **119**, 691 (2000).
- ³⁶ Y. Kopelevich, S. Moehlecke, and R. R. da Silva (Elsevier Science, 2006), chap. 18, in *Carbon-Based Magnetism*, T. Makarova and F. Palacio (Eds.), an refs. therein.
- ³⁷ I. Felner, E. Galstyan, B. Lorenz, D. Cao, Y. S. Wang, Y. Y. Xue, and C. W. Chu, Phys. Rev. B **67**, 134506 (2003).
- ³⁸ Y. Lu, M. Muñoz, C. S. Steplecaru, C. Hao, M. Bai, N. García, K. Schindler, and P. Esquinazi, Phys. Rev. Lett. **97**, 076805 (2006), see also the comment by S. Sadewasser and Th. Glatzel, Phys. Rev. Lett. **98**, 269701 (2007) and the reply by Lu et al., *idem* **98**, 269702 (2007); R. Proksch, Appl. Phys. Lett. **89**, 113121 (2006).
- ³⁹ N. B. Kopnin and E. B. Sonin, Phys. Rev. Lett. **100**, 246808 (2008).
- ⁴⁰ B. Uchoa and A. H. C. Neto, Phys. Rev. Lett. **98**, 146801 (2007).
- ⁴¹ A. M. Black-Schaffer and S. Doniach, Phys. Rev. B **75**, 134512 (2007).